

## Thermal behaviour of redeposited layer under high heat flux exposure

E. Gauthier<sup>a,\*</sup>, S. Dumas<sup>a</sup>, J. Matheus<sup>a</sup>, M. Missirlian<sup>a</sup>,  
Y. Corre<sup>a</sup>, L. Nicolas<sup>b</sup>, P. Yala<sup>b</sup>, P. Coad<sup>c</sup>, P. Andrew<sup>c</sup>,  
S. Cox<sup>c</sup>, the JET-EFDA contributors

<sup>a</sup> Association EURATOM-CEA, CEA/DSM/DRFC, CEA Cadarache, 13108 Saint Paul Lez Durance, France

<sup>b</sup> CEA Saclay, DEN/DM2S, 91191 Gif sur Yvette, France

<sup>c</sup> Euratom/UKAEA Fusion Association, Culham Science Centre, Abingdon OX14 3DB, UK

### Abstract

Power flux deposition during ELMs and disruptions needs to be controlled in ITER to avoid damage to the plasma facing components (PFC). In present tokamaks, the power and energy deposited on tiles during ELMs is calculated from the surface temperature measurements which are affected by the presence of deposited layers. The thermal behaviour of deposited layers under high heat load exposure has been investigated and the thermal properties of the layers have been determined from experimental data and modelling results obtained with the CAST3M code.

© 2004 Elsevier B.V. All rights reserved.

PACS: 52.40.Hf; 52.70.-m; 28.52.-s; 07.20.-n

Keywords: Power deposition; JET; Erosion deposition; Thermography; Divertor material

### 1. Introduction

Heat load deposition during transient events such as ELMs and disruptions is a critical issue for ITER. In the present ITER design, very different materials such as tungsten, carbon and beryllium are used as plasma facing components (PFC), and are distributed at different locations depending on the plasma wall interaction, and in particular on the heat load deposition, expected during ELMs. Thus, power and energy flux impinging

on the PFC during ELMs and disruptions need to be measured in tokamaks in order to validate the ITER material choice. In present tokamaks, power flux is usually deduced from surface temperature measurements using infrared cameras, and energy is deduced from temperature rise measured by thermocouples inserted in the bulk of the PFC. Unfortunately, the response of thermocouples is slow, due to the long time constant ( $\tau = l^2/D$ , where  $l$  is the distance between the thermocouple location and the surface of the tile and  $D$  the thermal diffusivity of the material). Thus transient events such as ELMs with durations in the range of 100–400  $\mu$ s in JET, cannot be resolved and energy impinging on the divertor cannot be measured with thermocouples for an individual ELM. Moreover, due to carbon layer

\* Corresponding author. Tel.: +33 225 4204; fax: +33 225 4990.

E-mail address: [eric.gauthier@cea.fr](mailto:eric.gauthier@cea.fr) (E. Gauthier).

deposition on the tile occurring during plasma operation, the surface temperatures are higher than expected on the initial material [1]. Additionally, the carbon layers are not homogeneously distributed on the tiles and these effects introduce large uncertainties in the power flux calculated from the surface temperature changes. In order to characterize the thermal behaviour of the PFC with carbon layers, experiments under high heat load have been conducted on divertor MkIIa tiles using the JET Neutral Beam Test Bed Facility. In the following sections, we will describe the experimental set-up and the numerical model, and results of low and high power flux exposures will be presented and discussed.

## 2. Experimental set-up

Carbon fibre composite (CFC) tiles covered with deposited layers have been placed at the centre line of the JET Neutral beam Test Bed in the Beryllium Rig at a distance of 2.9 m from the beam source. Experiments have been conducted on an inner (tile 4) and an outer tile (tile 7) of the MKIIa divertor. These tiles have been exposed to JET plasma during the 1995 and 1996 campaigns. Surface analysis of divertor tiles in the MKII-GB divertor indicated that the thickness of the deposited layer can be up to  $90\ \mu\text{m}$  [2]. Due to beryllium evaporation performed in JET, the tiles are beryllium contaminated, and films in some areas can have as large a Be/C ratio as unity [3].

Both tiles were exposed to particle beams with peak power density ranging between  $5\ \text{MW}/\text{m}^2$  and  $100\ \text{MW}/\text{m}^2$ , with pulse durations between 10 ms and 2 s. The power density distribution is usually measured by an *in situ* inertial calorimeter. Unfortunately, due to technical problems, the power density distribution could not be measured and has been obtained from simulation of the neutral beam parameters and from previous experiments on the test bed, performed in similar conditions. Deuterium and helium beams have been used for comparison. However, which gas was used made no noticeable difference to the results.

The CFC bulk temperature is measured by means of 12 thermocouples inserted at different depths from 5 to 20 mm from the surface, in order to evaluate the thermal diffusivity and the total energy deposited in the tile. Surface temperature is measured by using an infrared camera with a time resolution of 20 ms. A CCD camera is also used for visible observation.

## 3. Numerical model

A detailed 3-D model with true geometry of the tiles, taking into account the inconel dumbbell, was developed using the CAST3M code (finite element code developed

at CEA [4]) to calculate the surface and in-depth temperature distribution. Thermal properties of the CFC have been measured on samples taken from the batches of CFC used to manufacture the MKIIa tiles [5]. Thermal conductivity parallel and perpendicular to the CFC weave, and specific heat capacity are temperature dependent and are taken from reference [6]. A deposited layer, with a thickness of  $40\ \mu\text{m}$ , taken as an average, has been introduced in the model. The adjustable parameters are the thermal conductivity of the layer (assumed to be isotropic) and the heat exchange coefficient between the layer and the bulk material. The initial temperature is assumed to be uniform (this is confirmed with the different thermocouples) and is adjusted to the real initial temperature for the pulse. The power flux is applied on the upper tile surface with known time dependence. Radiative cooling to an environment at  $20\ ^\circ\text{C}$  is considered for all the surfaces of the tile. Two heat load conditions have been applied in the simulations:

- a low power density case with a  $5\ \text{MW}/\text{m}^2$  flux density during 2 s on and 2 s off for 3 cycles;
- a high power density case with a  $50\ \text{MW}/\text{m}^2$  flux density during 17 ms on and 43 ms off for 10 cycles.

Fig. 1 is a schematic view of the model and the time dependence of the flux for the low power case.

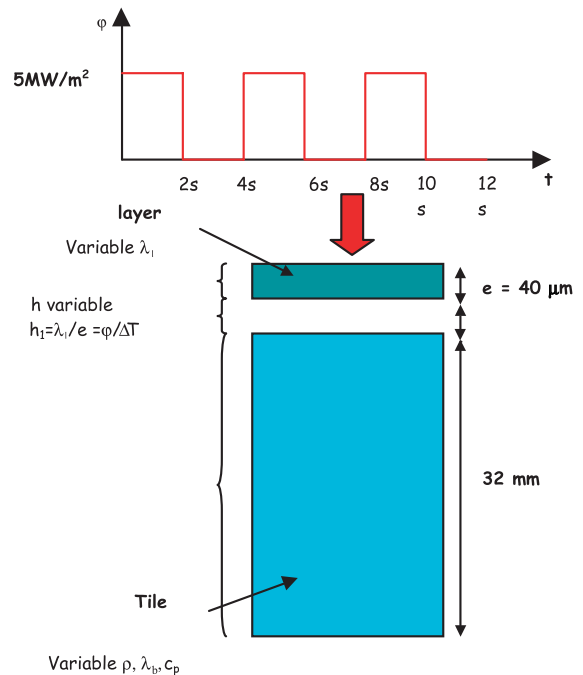


Fig. 1. Schematic view of the model and of the power flux.

#### 4. Results and discussion

First experiments have been conducted at a peak power flux of  $5 \text{ MW/m}^2$  during 3 cycles of 2 s. Preliminary simulations using bulk material properties without a layer predicted an increase of the surface temperature in the range of  $350 \text{ }^\circ\text{C}$  per cycle with a maximum temperature of  $900 \text{ }^\circ\text{C}$  reached at the end of the third pulse. The thermogram (infrared image) acquired during the beam exposure is shown in Fig. 2(a), and exhibits a completely different behaviour to that expected with a quasi-uniform power flux deposition [7]. Two parallel vertical lines along the direction of the tile (which corresponds also to the toroidal magnetic field direction when the tile was in the tokamak) can be observed and present much higher temperature than the rest of the tile. This image has been obtained 40 ms ( $\pm 20$  ms) after the beginning of the heat pulse. At this time, the increase of surface temperature  $\delta T$  on a bulk CFC material should be less than  $40 \text{ }^\circ\text{C}$ , whilst  $\delta T$  ranging between  $170 \text{ }^\circ\text{C}$  and  $460 \text{ }^\circ\text{C}$  are measured on the different points of the tile. This behaviour is typical of what is observed on the JET divertor during the power step discharges [8]. On this image, there is also a very obvious stripe across the image and a less distinct stripe near the bottom edge. These stripes correspond to areas where tape tests were performed during the surface analysis campaign [9]. Adhesive tape is stuck on the surface then peeled off, removing loosely adhered material. The test was

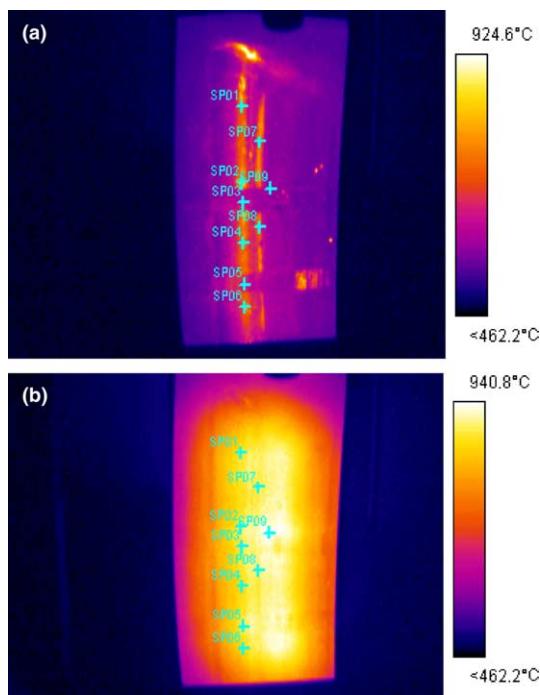


Fig. 2. Surface temperature during (a) and after (b) power flux exposure.

repeated several times at one of the stripes, and every time the tape came off with more adherent black carbon dust. Although no absolute measurement was done, probably tens of microns of carbon layer were removed from this stripe in the middle of the tile.

When the beams are switched off, the surface temperature steps down also very rapidly with the same time constant ( $<40$  ms) and then the surface temperature reflects the footprint of the neutral beam power flux distribution, as shown in Fig. 2(b).

Modelling the temperature evolution of the tile with no additional layer, and changing only the thermal properties of the CFC ( $\rho, \lambda_b, C_p$ ), cannot reproduce either the thermocouple or the surface temperature measurements. Using the thermal properties from reference [6], modelling data fit well the thermocouple measurements, as shown in Fig. 3(a), confirming the value of the thermal properties measured for the CFC. It should be noted that in many cases in our experiments several thermocouples did not respond correctly due to a bad thermal contact with the tile. Even though the time evolution could not be used in such a case, the temperature equilibrium, achieved about 30 s after the pulse, was measurable and allowed the total energy deposited on the tile to be calculated. The surface temperatures evolution measured at different locations on the tile are plotted on Fig. 3(b). Simulations have been performed with an additional carbon layer of  $40 \mu\text{m}$  with density and specific heat similar to the bulk values. The thermal conductivity  $\lambda_l$ , was set at 10% of the CFC and the heat exchange coefficient was varied between 5 and  $50 \text{ kW/m}^2 \text{ K}$ . Fig. 3(c) shows the surface temperature evolution calculated with CAST3M for a heat exchange coefficient of 20 and  $50 \text{ kW/m}^2 \text{ K}$  and, for comparison, without an additional layer. The curves reproduce very well both the amplitude and the time constant of the experimental temperatures. Nevertheless, it should be pointed out that the inverse problem of the heat conduction is a problem including more variables than experimental parameters and therefore a unique solution cannot be found [10]. In particular, it not possible to determine from such experiments all the relevant parameters which are: thickness, density, thermal conductivity, heat capacity of the layer and heat exchange coefficient between the bulk and the layer. For instance, the offset of the surface temperature compared with the bulk material can be attributed to a combination of two conductances:

$$1/h_{\text{eq}} = 1/h + 1/h_1, \quad (1)$$

where  $h$  is the heat exchange between the layer and the bulk and  $h_1$  is the heat exchange in the layer itself, defined by

$$h_1 = \lambda_l/e, \quad (2)$$

where  $e$  is the thickness of the layer. From the analysis of the simulated and experimental data, we can deduce that

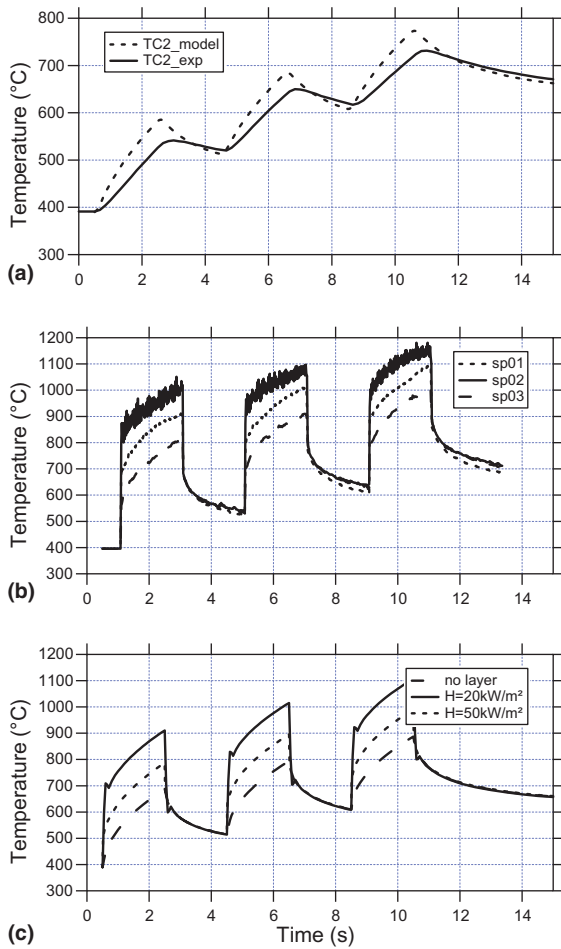


Fig. 3. Experimental and modelled temperature evolution at a thermocouple location (a), experimental values of surface temperature evolution at three points (sp01, sp02 and sp03 on Fig. 2) on the tile (b), and modelled values of surface temperature (c), for  $\phi = 5 \text{ MW/m}^2$  flux exposure (2 s on /2 s off; 3 cycles).

the equivalent heat exchange coefficient  $h_{eq}$  on different points is between 15 and  $50 \text{ kW/m}^2 \text{ K}$ . Other sets of parameters for  $\lambda$ ,  $\rho$ ,  $e$ ,  $C_p$  and  $h$  can produce the same value of  $h_{eq}$  and this does not imply that the layer is really  $40 \mu\text{m}$  thick.

In addition to the offset, the rise time of the surface temperature gives also information on the thermal properties of the layer. When the power flux  $\phi$ , is applied, the average temperature,  $\bar{T}$  in the layer is governed by

$$\epsilon\rho C_p \frac{\partial \bar{T}}{\partial t} = \phi - h\bar{T} \quad (3)$$

and the time constant of the temperature increase in the layer,  $\tau$  is:

$$\tau = \frac{\epsilon\rho C_p}{h} \quad (4)$$

Using the parameters introduced in the code, we obtained  $\tau = 2.6 \text{ ms}$ , in agreement with the experimental observation. Higher time resolution would be required to measure precisely the time constant and consequently the ratio  $\epsilon\rho h$  ( $C_p$ , being known).

Experiments with high heat load exposure at  $50 \text{ MW/m}^2$  during 10 ms for 10 cycles have also been performed in similar conditions. Due to the short length and the frequency of the pulses (17 Hz), the thermocouples could not resolve the individual heat pulses. Nevertheless, the equilibrium temperature achieved about 20 s after the end of the power flux exposure gives an accurate measurement of the energy deposited on the tile. Simulations (with the same parameters as the low power case) still show very good agreement with the thermocouples data. The experimental and stimulated surface temperature evolution at different location on the surface are plotted on Fig. 4. Since the power flux duration is smaller than the acquisition rate of the IR camera, only one measurement could be acquired per pulse. On the deposited layer, the temperature reaches more than  $2000 \text{ }^\circ\text{C}$  at the first pulse and  $\sim 2300 \text{ }^\circ\text{C}$  at the tenth pulse while it varies only from  $800 \text{ }^\circ\text{C}$  to  $1200 \text{ }^\circ\text{C}$  at other locations on the tile. Both simulated curves in Fig. 4 (i.e. bulk, and bulk plus layer, with heat exchange coefficient of  $50 \text{ kW/m}^2 \text{ K}$ ) fit the experimental results very well.

An additional feature has been observed during the experiments at high power. The tile was exposed to several identical shots, and it was noticeable that the maximum temperature decreased slightly with the shot number. Fig. 5 shows a 2-D map of differences in the temperatures achieved at the end of two similar shots, performed at an interval of a few days. The areas of significant temperature differences correspond to areas with deposited layers. This variation in the surface temperature, of up to  $500 \text{ }^\circ\text{C}$ , is due to the modifications of the surface layer properties. Erosion can be excluded, due to the high energy of the

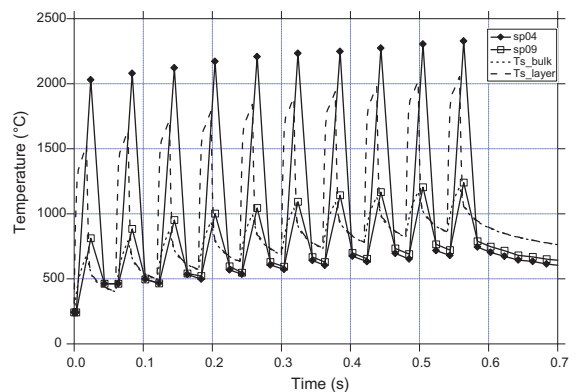


Fig. 4. Experimental and modelled Surface temperature evolution at two points (sp04 and sp09 on Fig. 2), for  $\phi = 50 \text{ MW/m}^2$  flux exposure (17 ms on /43 ms off; 10 cycles).

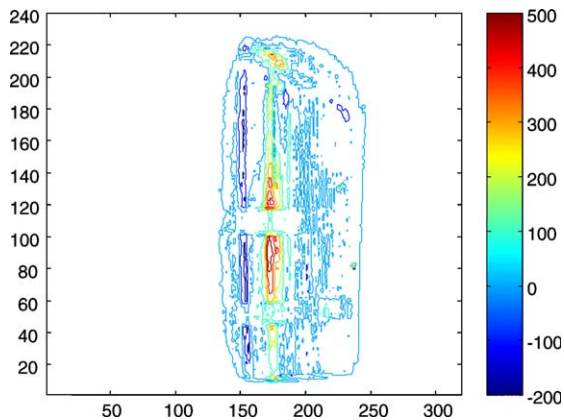


Fig. 5. Surface temperature variation for two similar shots ( $\varphi = 50 \text{ MW/m}^2$ ), induced by modifications of the thermal properties of the surface layer.

incoming particles (130 keV), and sublimation of carbon at  $2300 \text{ }^\circ\text{C}$  could not explain such a large effect within such a very limited time ( $\sim 10 \text{ s}$ ). Therefore, this variation in the surface temperature is probably due to annealing of the layer at high temperature, inducing structural modification (graphitisation) and enhancement of the thermal properties of the deposited layer. This change in the properties of the deposited layer with time adds further complexity to the system, and will introduce additional uncertainties in the determination of the power flux from surface temperature changes.

## 5. Conclusion

The thermal behaviour of deposited layers under power flux exposure has been characterized by using

the JET Neutral beam test bed. Surface and thermocouple temperatures have been successfully modelled using CAST3M code, by including an additional layer with low thermal conductivity, and a heat exchange coefficient between the bulk and the layer. The deposited layer is non-uniform, and a unique heat exchange coefficient cannot reproduce the 2D surface temperature. Heat exchange coefficients were estimated from modelling results and experimental data, and values range between  $15$  and  $50 \text{ kW/m}^2 \text{ K}$ . The thickness of the layer (in fact the product:  $e\rho C_p$ ) can also be estimated but require surface temperature measurements with time resolution lower than  $1 \text{ ms}$ . Modifications of the thermal properties of the layer occur when the temperature exceeds  $2000 \text{ }^\circ\text{C}$ . There are large uncertainties in the power flux calculated from surface temperature measurements under such conditions.

## References

- [1] E. Gauthier et al., in: Proc. of 24th EPS Conf., 21A, 61 (1997).
- [2] J.P. Coad et al., J. Nucl. Mater. 313–316 (2003) 419.
- [3] M. Rubel et al., J. Nucl. Mater. 313–316 (2003) 321.
- [4] CAST3M, see <http://www-cast3m.cea.fr>.
- [5] H. Altmann et al., in: Proc. of the 16th SOFE, 1995.
- [6] V. Riccardo et al., PPCF 23 (2001).
- [7] J. Matheus, E. Gauthier, M. Missirlian, note CEA CFP/NTT-2002-027 (2002).
- [8] Y. Corre et al., in: 30th EPS Conference, St. Petersburg, 2003.
- [9] J.P. Coad, private communication, 2003.
- [10] C. Martinsons, M. Heuret, High Temp.–High Pressures 31 (1999) 99.